NOTES ON NUMERICAL FLUID MECHANICS AND MULTIDISCIPLINARY DESIGN · VOLUME 116

Fundamental Medical and Engineering Investigations on Protective Artificial Respiration

A Collection of Papers from the DFG Funded Research Program PAR

Michael Klaas
Edmund Koch
Wolfgang Schröder (Eds.)

Springer

Fundamental Medical and Engineering Investigations on Protective Artificial Respiration

A Collection of Papers from the DFG Funded Research Program PAR

Michael Klaas, Edmund Koch,
and Wolfgang Schröder (Eds.)

Springer

Dr.-Ing. Michael Klaas
Lehrstuhl für Strömungslehre und
Aerodynamisches Institut
RWTH Aachen
Wüllnerstr. 5a
52062 Aachen
Tel.: ++49 (0) 241/80-95412
Fax: ++49 (0) 241/80-92257
E-mail: m.klaas@aia.rwth-aachen.de

Prof. Dr.-Ing. Wolfgang Schröder
Lehrstuhl für Strömungslehre und
Aerodynamisches Institut
RWTH Aachen
Wüllnerstr. 5a
52062 Aachen
Tel.: ++49 (0) 241/80-95410
Fax: ++49 (0) 241/80-92257
E-mail: office@aia.rwth-aachen.de

Prof. Dr. rer. nat. Edmund Koch
Arbeitsgruppe Klinisches
Sensoring und Monitoring
Medizinische Fakultät Carl
Gustav Carus
TU Dresden
Fetscherstr. 74
01307 Dresden
Tel.: ++49 (0) 351/458-6131
Fax: ++49 (0) 351/458-6325
E-mail: edmund.koch@tu-dresden.de

ISBN 978-3-642-20325-1 e-ISBN 978-3-642-20326-8

DOI 10.1007/978-3-642-20326-8

Notes on Numerical Fluid Mechanics
and Multidisciplinary Design ISSN 1612-2909

Library of Congress Control Number: 2011925862

Typeset & Cover Design: Scientific Publishing Services Pvt. Ltd., Chennai, India.

Printed on acid-free paper

5 4 3 2 1 0

springer.com

NNFM Editor Addresses

Prof. Dr. Wolfgang Schröder
(General Editor)
RWTH Aachen
Lehrstuhl für Strömungslehre und
Aerodynamisches Institut
Wüllnerstr. 5a
52062 Aachen
Germany
E-mail: office@aia.rwth-aachen.de

Prof. Dr. Kozo Fujii
Space Transportation Research Division
The Institute of Space
and Astronautical Science
3-1-1, Yoshinodai, Sagamihara
Kanagawa, 229-8510
Japan
E-mail: fujii@flab.eng.isas.jaxa.jp

Dr. Werner Haase
Höhenkirchener Str. 19d
D-85662 Hohenbrunn
Germany
E-mail: office@haa.se

Prof. Dr. Ernst Heinrich Hirschel
(Former General Editor)
Herzog-Heinrich-Weg 6
D-85604 Zorneding
Germany
E-mail: e.h.hirschel@t-online.de

Prof. Dr. Ir. Bendiks Jan Boersma
Chair of Energytechnology
Delft University of Technology
Leeghwaterstraat 44
2628 CA Delft
The Netherlands
E-mail: b.j.boersma@tudelft.nl

Prof. Dr. Michael A. Leschziner
Imperial College of Science
Technology and Medicine
Aeronautics Department
Prince Consort Road
London SW7 2BY
U.K.
E-mail: mike.leschziner@ic.ac.uk

Prof. Dr. Sergio Pirozzoli
Università di Roma “La Sapienza”
Dipartimento di Meccanica e Aeronautica
Via Eudossiana 18
00184, Roma, Italy
E-mail: sergio.pirozzoli@uniroma1.it

Prof. Dr. Jacques Periaux
38, Boulevard de Reuilly
F-75012 Paris
France
E-mail: jperiaux@free.fr

Prof. Dr. Arthur Rizzi
Department of Aeronautics
KTH Royal Institute of Technology
Teknikringen 8
S-10044 Stockholm
Sweden
E-mail: rizzi@aero.kth.se

Dr. Bernard Roux
L3M – IMT La Jetée
Technopole de Chateau-Gombert
F-13451 Marseille Cedex 20
France
E-mail: broux@l3m.univ-mrs.fr

Prof. Dr. Yurii I. Shokin
Siberian Branch of the
Russian Academy of Sciences
Institute of Computational
Technologies
Ac. Lavrentyeva Ave. 6
630090 Novosibirsk
Russia
E-mail: shokin@ict.nsc.ru

Foreword

In 2005 the German Research Association DFG launched the research program "Protective Artificial Respiration" which is a joint initiative of medicine and fluid mechanics. The main long-term objective of this program is the development of a more protective artificial respiratory system to reduce the physical stress of patients undergoing artificial respiration. To satisfy this goal 11 projects have been defined. In each of these projects scientists from medicine and fluid mechanics do collaborate in several experimental and numerical investigations to improve the fundamental knowledge on respiration and to develop a more individual artificial breathing concept.

This volume contains the papers presented at the "2nd Aachen Symposium on Natural and Artificial Respiration" held at the "Erholungs-Gesellschaft Aachen 1837" in Aachen, Germany on November, 23 – 24, 2009. The symposium was organized by the Institute of Aerodynamics, RWTH Aachen University, Germany.

Numerous visiting scientist contributed to the success of this research program, namely Ben Fabry (University of Erlangen, Erlangen, Germany), Samir N. Ghadiali (The Ohio State University, Columbus/OH, USA), Göran Hedenstierna (University Hospital, Uppsala, Sweden), Rof Hubmayr (Mayo Clinic, Rochester/MN, USA), Oliver Jensen (The University of Nottingham, Nottingham, UK), Christian Kähler (Universität der Bundeswehr München, Neubiberg, Germany), Ching-Long Lin (University of Iowa, Iowa City/IA, USA), Ralph Lindken (TU Delft, Delft, Netherlands), Young Moon (Korea University, Seoul, Korea), Paolo Pelosi (University of Insubria, Varese, Italy), Christian Putensen (University Hospital Bonn, Bonn, Germany), Michael Quintel (Georg-August-University of Göttingen, Göttingen, Germany), Peter Schmid (Ecole Polytechnique, Palaiseau, France), Arthur .S. Slutsky (St. Michael's Hospital, Toronto, Canada), Christian Stemmer (TU München, Munich, Germany), Bela Suki (Boston University College of Engineering, Boston/MA, USA), and Marcos F. Vidal Melo (Harvard Medical School, Boston/MA, USA). In the name of all scientists involved in the research program „Protective Artificial Respiration", the speakers of the program, Edmund Koch (TU Dresden, Germany) and Wolfgang Schröder (RWTH Aachen University, Aachen Germany), would like to express gratitude to all the visiting scientists for their contributions.

The present monograph is a snapshot of the state-of-the-art of the joint initiative of medicine and engineering to develop new ventilation systems. The volume gives a broad overview of the ongoing work in this field in Germany. The order of the papers in this book corresponds closely to that of the sessions of the Symposium.

The editors are grateful to Prof. Dr. W. Schröder as the General Editor of the "Notes on Numerical Fluid Mechanics and Multidisciplinary Design" and to the Springer-Verlag for the opportunity to publish the results of the Symposium.

December 2010

M. Klaas, Aachen
E. Koch, Dresden
W. Schröder, Aachen

Contents

Advanced Multi-scale Modelling of the Respiratory System

Lena Wiechert, Andrew Comerford, Sophie Rausch, and Wolfgang A. Wall

Abstract. This chapter is concerned with computational modelling of the respiratory system against the background of acute lung diseases and mechanical ventilation. Conceptually, we divide the lung into two major subsystems, namely the conducting airways and the respiratory zone. Due to their respective complexity, both parts are out of range for a simulation resolving all relevant length scales. Therefore, we develop novel multi-scale approaches taking into account the unresolved parts appropriately. In the respiratory zone, an alveolar ensemble is modelled considering not only tissue behaviour but also the influence of the covering surfactant film. On the global scale, a homogenised parenchyma model is derived from experiments on living lung tissue. At certain hotspots, novel nested multi-scale procedures are utilised to simulate the dynamic behaviour of lung parenchyma as a whole while still resolving alveolar scales locally. In the tracheo-bronchial region, CT-based geometries are employed in fluid-structure interaction simulations. Physiological outflow boundary conditions are derived by considering the impedance of the unresolved parts of the lung in a fully coupled 3D-0D procedure. Finally, a novel coupling approach enables the connection of 3D parenchyma and airway models into one overall lung model for the first time.

1 Introduction

When compared to other areas in (computational) continuum biomechanics, like the circulatory or the muscosceletal system, research on the respiratory system is only in its infancy. This is quite astonishing especially when considering the huge impact a better understanding of respiratory mechanics can offer. A sound standing "virtual lung model" could be a valuable tool for

Lena Wiechert · Andrew Comerford · Sophie Rausch · Wolfgang A. Wall
Institute for Computational Mechanics
e-mail: {wiechert,comerford,rausch,wall}@lnm.mw.tum.de

M. Klaas et al. (Eds.): Fundamental Medical and Engineering Invest. on PAR, NNFM 116, pp. 1–32.
springerlink.com

various applications ranging from the better understanding of lung diseases to progress on individual therapeutic approaches.

Within the "Protective Artificial Respiration" program, we are interested in improving the treatment of patients suffering from the Acute Respiratory Distress Syndrome (ARDS). This severe diffuse lung disease is characterised by a number of symptoms such as reduced overall lung compliance, edema, severe hypoxemia and general inflammation of the lung parenchyma. Although many therapeutic approaches have been developed, the mortality associated with ARDS remains relatively high (Tsushima et al. 2009). An indispensable tool in the treatment for ARDS is mechanical ventilation. However, heterogeneity of the ARDS lung predisposes patients towards a number of associated complications which are collectively termed ventilator induced lung injuries (VILI) and deemed one of the most important factors in the pathogenesis of ARDS (Ranieri et al. 1999). VILI mainly occurs at the alveolar level of the lungs in terms of primary mechanical and secondary inflammatory injuries (DiRocco et al. 2005). Primary injuries are consequences of alveolar overexpansion or frequent recruitment and derecruitment inducing high shear stresses. Since mechanical stimulation of cells can result in the release of proinflammatory mediators – a phenomenon commonly called mechanotransduction – secondary inflammatory injuries often directly follow, possibly starting a cascade of events leading to sepsis or multi-organ failure. Understanding the reason why the lungs still become damaged or inflamed despite recent developments towards more "protective" ventilation protocols (Amato et al. 1998) is a key question sought by the medical community.

Computational models of the respiratory system can provide essential insights into the involved phenomena and open up new vistas towards improved patient-specific ventilation protocols. However, the lung comprises 23 generations of dichotomously bifurcating airways ending in approximately 300 million alveoli. This complexity inhibits a direct numerical simulation resolving all levels of the respiratory system from the onset. Therefore, we first develop detailed models for distinct parts of the lung. However, for our models to be of clinical significance, the regions not modelled explicitly must also be taken into account. Therefore, we have established advanced multi-scale approaches, which connect the individual detailed models, allowing for the simulation of the entire lung. Since our methods are built up from "first principles", the developed model will be applicable to a wide spectrum of problems and diseases.

The work described in the following was realised in our in-house finite element (FE) software platform BACI covering a wide range of applications in computational mechanics, like e.g. multi-field and multi-scale problems, structural and fluid dynamics, material modelling and finite element technology.

2 Computational Model of Pulmonary Alveoli

Since pulmonary alveoli are the main site of VILI, a detailed knowledge of all involved phenomena is crucial in order to obtain insights in the underlying

mechanisms. To this end, it is not only necessary to investigate alveolar soft tissue characteristics but also the influence of the alveolar liquid lining on the overall mechanical behaviour.

Previous models usually focused on only one of these two aspects. In Dale et al. (1980), an alveolus was modelled as a network of fibres without considering either the effect of interfacial phenomena or an underlying ground substance. Some subsequent approaches based on the work of Kowe et al. (1986) retained the idea of reducing alveolar soft tissue to a network of fibres while additionally considering surface stresses due to the liquid lining. Other attempts concentrated on the modelling of tissue mechanics whereas interfacial phenomena were treated in a simplified manner or even totally neglected as presented in Karakaplan et al. (1980) or Gefen et al. (2001), respectively. Contrary to the mentioned former approaches, our alveolar model introduced in the following combines a detailed constitutive law for alveolar soft tissue with an elaborate dynamic surface stress model.

2.1 Modelling of Alveolar Tissue

Alveolar tissue consists of three layers, the epithelial monolayer of alveolar type I and type II cells, the basal layer comprising the fibre network and – depending on the location – the interstitium or endothelial layer of blood vessels. According to Suki et al. (2005), the fibre network itself is composed of mechanically dominant collagen I as well as collagen III, elastin and proteoglycans. It was shown in Yuan et al. (1997) that the contribution of interstitial cells to alveolar mechanics seems to be marginal and the macroscopic elastic and dissipative properties are dominated by both collagen and elastin. Experimental results presented e.g. in Toshima et al. (2004) suggest that lung tissue can be treated as a homogeneous, isotropic continuum.

Assuming a hyperelastic material behaviour, the existence of a strain-energy function (SEF) can be postulated

$$W := W(\bar{I}_1, I_3) = W_{\text{vol}}(I_3) + W_{\text{iso}}(\bar{I}_1) \tag{1}$$

with W_{vol} denoting the volumetric and W_{iso} representing the isochoric part. I_3 and $\bar{I}_1$ denote the third and modified first invariant of the right Cauchy-Green deformation tensor $\boldsymbol{C}$ given by

$$I_3 := \mathsf{det}\mathbf{C}, \quad \bar{I}_1 := I_3^{-1/3}\mathsf{tr}\mathbf{C}. \tag{2}$$

Since the constituents of alveolar tissue exhibit different mechanical properties, a material model capable of distinguishing the corresponding contributions to the overall energy seems particularly suitable. Following the approach introduced for arterial tissue in Holzapfel et al. (2000), our isochoric part of the SEF therefore consists of two main parts related to the major stress-bearing elements in alveolar walls. The first contribution representing mainly

ground substance and the elastin fibre network is given as follows

$$W_{\text{iso}}^{\text{gs}}(\bar{I}_1) = c\left(\bar{I}_1 - 3\right) \tag{3}$$

with $c > 0$ being a shear-modulus-like parameter.

The second contribution to the isochoric SEF is related to the collagen fibre network. Assuming an isotropic distribution of fibre orientations, the corresponding part reads

$$W_{\text{iso}}^{\text{fib}}(\bar{I}_1) = \begin{cases} \frac{k_1}{2k_2}\left[exp\left[k_2\left(\frac{1}{3}\bar{I}_1 - 1\right)^2\right] - 1\right] & \text{for } \bar{I}_1 \geq 3 \\ 0 & \text{for } \bar{I}_1 < 3 \end{cases} \tag{4}$$

following Delfino et al. (1997) with $k_1 \geq 0$ as a stress-like parameter and $k_2 > 0$ as a dimensionless parameter. Hence, collagen fibres contribute to the overall potential only in case of tension.

Since soft biological tissues are commonly known to be quasi-incompressible, a penalty function enforcing this constraint locally is used for the volumetric part of the SEF. It is noteworthy that each part of the SEF fulfils the principles of objectivity and material symmetry as well as the requirements of polyconvexity and a stress-free reference state. More details on the employed constitutive models can be found in Wiechert et al. (2009).

Unfortunately, reliable material parameters for single alveolar walls are currently unavailable. Therefore, we fitted our constitutive model to experimental data obtained for lung tissue strips in Al Jamal et al. (2001) as a first step. Consequently, the chosen parameters model a homogenised continuum of alveolar tissue and air rather than a single alveolar interseptum. However, we currently work on deriving parameters for the alveolar wall by resolving the micro-structure of the tested tissue strips in an inverse analysis as presented in section 3.

2.2 Modelling of Alveolar Liquid Lining

Pulmonary alveoli are covered by a thin continuous aqueous film with a monomolecular layer of surface active agents – the so-called surfactant – on top of it (Bastacky et al. 1995). This surfactant layer contributes to alveolar stability at low lung volumes and reduces the work of breathing significantly.

In general, molecules at an interface are in an energetically unfavourable state compared to those in the bulk due to reduced intermolecular attraction. As a consequence, surface stresses arise that tend to minimise surface area and, thus, interfacial energy. In case of ideal liquids such as water, these surface stresses are constant. By contrast, surface stresses of a surfactant layer depend on the local surfactant concentration. During breathing, the liquid lining periodically expands and contracts, resulting in a periodic variation of surfactant concentration and therefore also surface stresses.

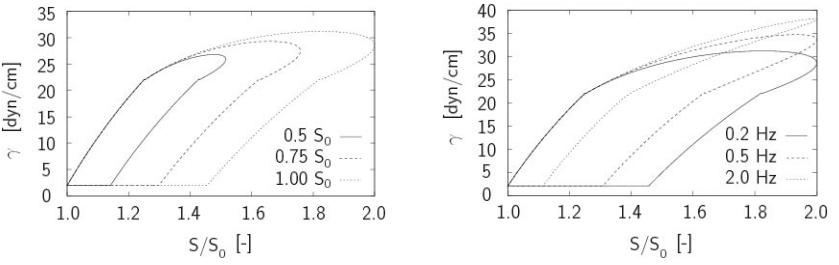

Fig. 1 Non-linear and time-dependent behaviour of surfactant model for sinusoidal change of interfacial area S. Left: Different amplitudes. Right: Different frequencies.

To capture this particular behaviour, we employ the surfactant constitutive model introduced in Otis et al. (1994). Briefly, current surfactant concentrations Γ are calculated by modelling transport between bulk fluid and interface. An isothermal relationship is then used to determine local surface stresses, which depend nonlinearly and dynamically on the current interfacial area.

In the first regime, Γ is less than the maximum equilibrium concentration Γ^* and surfactant transport is governed by Langmuir kinetics. The temporal development of Γ depending on the interfacial area S is given by

$$\frac{\mathrm{d}}{\mathrm{d}t}\left(\frac{\Gamma}{\Gamma^*}S\right) = S\left[k_1 C\left(1-\frac{\Gamma}{\Gamma^*}\right) - k_2\frac{\Gamma}{\Gamma^*}\right] \tag{5}$$

with k_1 and k_2 being the adsorption and desorption coefficient, respectively, whereas C denotes the bulk concentration of surfactant molecules in the hypophase. The corresponding current surface stress is related to the surfactant concentration via the following linear isotherm

$$\gamma = \gamma_0 - m_1\frac{\Gamma}{\Gamma^*} \tag{6}$$

where γ_0 is the reference surface tension of water and m_1 is the experimentally derived isotherm slope for the first regime.

In the second regime ($\Gamma^* \leq \Gamma < \Gamma_{\max}$), the monolayer is modeled as insoluble. Consequently, no mass transport of surfactant takes place and the concentration changes merely due to variations of interfacial area. Again, surface stresses can be calculated with the help of a linear isotherm according to

$$\gamma = \gamma^* - m_2\left(\frac{\Gamma}{\Gamma^*} - 1\right) \tag{7}$$

with γ^* being the minimum equilibrium surface stress and m_2 denoting the isotherm slope for the second regime.

In the third regime, Γ equals the maximum surfactant concentration $\Gamma_{\max}$ and accordingly minimum surface stress $\gamma_{\min}$ is reached. Any further decrease in interfacial area results in a 'squeeze-out' of molecules.

In Figure 1, plots are shown illustrating the course of γ for different frequencies and amplitudes if interfacial area is changed sinusoidally.

Instead of modelling the thin liquid lining explicitly, we confine ourselves to considering the interfacial energy of the surfactant layer only. An isolated surface stress element as e.g. proposed in Kowe et al. (1986), however, degenerates to an ideal point without appropriate boundary conditions. It seems more sensible to establish a direct coupling between bulk and interface mechanics. Therefore, we incorporate the additional interfacial energy of the surfactant layer into the surfaces of standard structural finite elements representing the alveolar wall.

Due to the small thickness of the liquid lining, the surface area of the surfactant-air interface and the alveolar wall are assumed to be identical. Consequently, we obtain for the overall work associated with a change in interfacial area

$$W_{\text{surf}} = \int_{S_0}^{S} \gamma \mathrm{d}S^* \tag{8}$$

with S_0 and S denoting initial and current interfacial area, respectively.

After discretising the interface in space, the variation of the overall work with respect to the nodal displacements $\mathbf{D}$

$$\delta W_{\text{surf}} = \left(\frac{\partial}{\partial S} \left(\int_{S_0}^{S} \gamma \mathrm{d}S^* \right) \frac{\partial S}{\partial \mathbf{D}} \right)^T \delta \mathbf{D} \tag{9}$$

finally yields

$$\delta W_{\text{surf}} = \gamma \left(\frac{\partial S}{\partial \mathbf{D}} \right)^T \delta \mathbf{D} = \mathbf{f}_{\text{surf}}^T \delta \mathbf{D} \tag{10}$$

with the force vector

$$\mathbf{f}_{\text{surf}} = \gamma \frac{\partial S}{\partial \mathbf{D}}. \tag{11}$$

The consistent tangent stiffness matrix is derived by linearisation of (11)

$$\mathbf{K}_{\text{surf}} = \gamma \frac{\partial}{\partial \mathbf{D}} \left(\frac{\partial S}{\partial \mathbf{D}} \right)^T + \frac{\partial \gamma}{\partial S} \frac{\partial S}{\partial \mathbf{D}} \left(\frac{\partial S}{\partial \mathbf{D}} \right)^T. \tag{12}$$

The derivative of the current local surface stresses with respect to the interfacial area can be determined in a straightforward manner based on the constitutive equations introduced previously.

In contrast to former approaches presented e.g. in Kowe et al. (1986) or Denny and Schroter (2000), our consistent continuum-mechanical formulation enables us to consider arbitrarily curved interfaces for the first time. More details can be found in Wiechert et al. (2009).

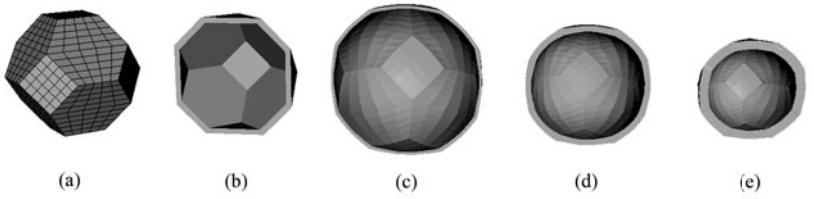

Fig. 2 Single artificial alveoli with different interfacial configurations under sinusoidally varying hydrostatic pressure ($p_{\max} = 600$Pa). (a) Undeformed geometry with mesh. (b) Section of undeformed geometry. (c)-(e) Sections of deformed geometries under maximum load in case of (c) tissue, (d) tissue coupled with surfactant and (e) tissue coupled with water film (each exaggerated 1.5 times).

Figure 2 shows first results of simulations combining interfacial effects with the presented material model for an artificial alveolar geometry. The observable differences in the overall deformation states affirm the importance of considering interfacial phenomena in alveolar mechanics. A comparison of the results for surfactant and water films demonstrates the efficiency of surfactant in decreasing the surface tension of the aqueous hypophase, hence reducing the overall stiffness of alveoli. Pathological changes in surfactant composition may thus result in severe alterations of alveolar mechanical behaviour. As illustrated by the exemplary simulations, this effect can inherently be taken into account in our model.

2.3 Geometric Representation

Alveolar tissue can be characterised as an irregular open foam consisting of mainly polyhedral structures with average dimensions ranging from 90 to 200μm depending on the species. Recently, micro-CT data for isolated fixed rat lung tissue became available (Schittny et al. 2008), allowing us to investigate realistic alveolar assemblages in detail for the first time.

Obviously, overstraining and inflammation of alveolar tissue is a highly local phenomenon. Hence, resolving the alveolar micro-structure and quantifying local stresses and strains in alveolar walls seems to be essential when investigating the effect of VILI. In preliminary studies presented in Rausch et al. (2010a), we studied the influence of local geometric features on the distribution of strains. A cube of lung tissue was segmented from CT data and meshed with recently developed tetrahedral elements (Gee et al. 2009) as shown in Figure 3(a). For our simulations, we prescribed simple global deformation states (Figure 3(b)) and calculated the local principal strains (Figure 3(c)). We found that local strains in alveolar walls are up to four times larger than the prescribed global ones. Consequently, resolving the realistic alveolar morphology is crucial when investigating local overstretching of lung tissue.

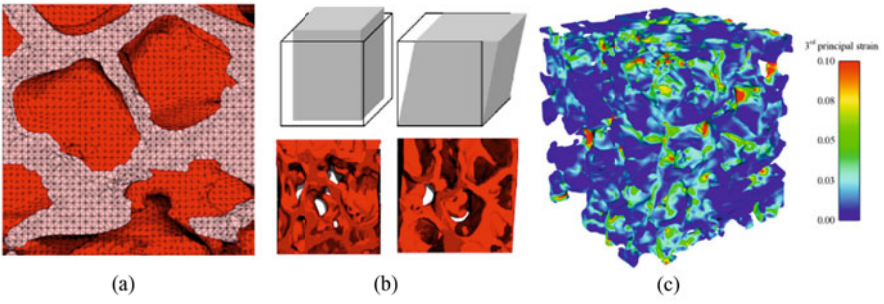

Fig. 3 Simulated deformation of a CT-based alveolar geometry. (a) Detail view of utilised finite element mesh. (b) Uniaxial tension and simple shear as "global" deformation states prescribed in the simulations. (c) Distribution of local third principal strains in case of global uniaxial stretch. Colours from blue to red indicate increasing strains.

However, due to the persisting limited availability of CT-based geometries – particularly for species other than rats –, we are interested in finding ways to generate simplified artificial alveolar representations. Furthermore, realistic geometries require elaborate FE meshes due to their complex irregularity. The simulation using the relatively small alveolar ensemble shown in Figure 3(c) already involves 8.6 million FE. Hence, by analysing general phenomena using CT-based geometries, we want to provide a basis for validating our simpler artificial models later on.

A well-established regular shape employed for the representation of artificial alveolar ducts and alveoli is the so-called tetrakaidecahedron or truncated octahedron, see e.g. Fung (1988) or Denny and Schroter (2000). We propose to connect these complex polyhedra to an artificial ventilatory unit by employing a modified version of the labyrinthine algorithm presented in Kitaoka et al. (2000) for cubic alveoli. Point of origin is an assemblage of identical space-filling and initially closed cells, in our case represented by tetrakaidecahedra. By successively opening faces, connections of all cells to an arbitrarily located starting cell are established. The employment of a set of geometry-dependent connection rules a priori guarantees minimal overall pathlength within the ensemble. Since this feature seems essential against the background of optimal gas exchange, the labyrinthine algorithm was deemed suitable to model the presumed physiological state.

Examples of created random pathways through an assemblage of 35 tetrakaidecahedra are depicted on the left hand side of Figure 4. For the sake of lucidity, the surrounding tetrakaidecahedra are left out and only the pathways connecting the cell centres are displayed.

On the right hand side of Figure 4, a calculated displacement distribution for an assemblage of 91 interconnected 3D alveoli under hydrostatic pressure is shown. Due to the regular shape, alveolar ensembles can be meshed with

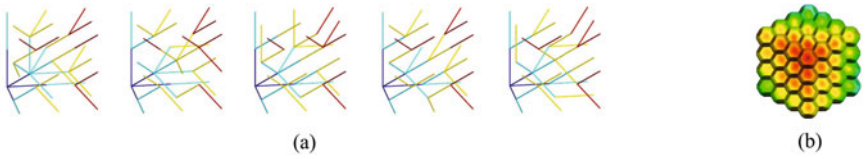

Fig. 4 (a) Random pathways through an assemblage of 35 tetrakaidecahedra. Colours indicate distances to the starting cell with blue denoting proximal and red meaning distal. (b) Ensemble of 91 interconnected alveoli under hydrostatic pressure. Colours from blue to red indicate increasing absolute displacements.

hexahedral elements exclusively. Overall, much less degrees of freedom are required for meshing a cube of the same size than the CT-based geometry presented before. However, the geometric representation is of course simplified here and the similarity of results – particularly the relation between global and local quantities – still needs to be shown.

Although alternative concepts for creating interalveolar connections exist in the literature (Denny and Schroter 1996), so far only simplified configurations were used for computational simulations (confer e.g. Denny and Schroter (1997, 2006); Kowe et al. (1986)). Therefore, to the authors' knowledge no other simulations based on advanced artificial acinar models – not to mention CT-based ones – have been done so far.

3 Computational Model of Lung Parenchyma

As indicated in the previous section, the simulation of small alveolar ensembles already becomes computationally very expensive. Hence, modelling all 300 million alveoli in the human lung is obviously not feasible. Therefore, we propose to employ novel multi-scale techniques to resolve the alveolar micro-structure at certain hotspots only and model lung parenchyma as a homogenised continuum otherwise. In the following, both complementary approaches will be briefly presented.

3.1 Homogenised Parenchyma Model

Although some experimental data on the mechanical behaviour of lung parenchyma can be found in literature, e.g. in Fukaya et al. (1968), Cavalcante et al. (2005) or Gao et al. (2006), the accuracy is often not adequate and detailed geometrical information, such as clamp location during testing, is missing. To feed our sophisticated models, therefore additional experimental studies are necessary. Hence, we have conducted uniaxial tension tests on living lung tissue prepared from isolated rat lungs as previously described (Martin et al. 1996). Briefly, rat lungs were dissected from the animal, filled with agarose solution und cut into 500μm thick tissue strips. After

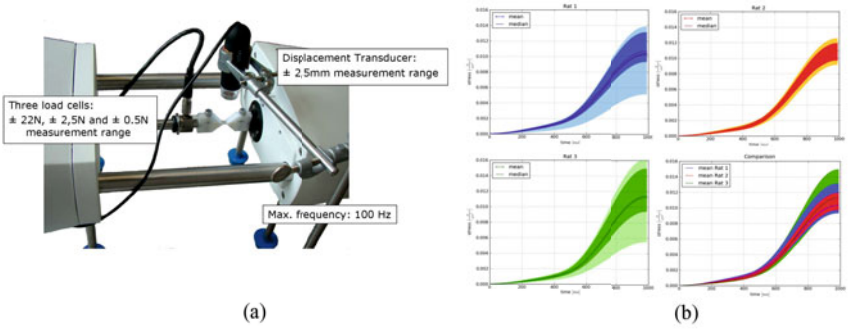

Fig. 5 Determination of material parameters for lung parenchyma. (a) Experimental set-up for uniaxial tension tests with the BoseElectroforce3100. (b) Experimentally determined stress curves. The first three plots show the distribution of different specimens dissected from one animal. The region characterised by the lighter colour is the confidence region of the percentile, the darker colour indicates the confidence region of the quartiles. The last plot compares the quartile confidence regions of three different rat lungs.

slicing, the agarose was washed out again. Previous tests have shown that these so-called precision-cut lung slices (PCLS) are viable for more than three days. Our experiments were performed within 48 hours after dissection of the lungs.

As a testing device, the Bose ElectroForce3100 is employed (force transducer with a range of ± 0.5N and a resolution of under 2.5mN, displacement transducer with a range of ± 2.5mm and a resolution of under 12.5μm, see Figure 5(a)). In a first step, we focus on the elastic properties of lung parenchyma. Hence, all tissue strips are preconditioned before testing in order to eliminate viscoelastic effects inherent to all soft biological tissues. Subsequently, the PCLS are cyclically stretched to determine their elastic material behaviour. Interestingly, the experimentally derived stress curves are very similar for both different specimens of one rat and specimens of different animals. A representative selection of stress plots can be found in Figure 5(b).

For the determination of a proper constitutive model and the corresponding material parameters, we perform a so-called inverse analysis based on the Levenberg-Marquardt Algorithm (Levenberg 1944; Marquardt 1963). Briefly, we simulate the experiment in silico for each chosen combination of SEF using varying material parameters until we obtain the optimal fit (see Figure 6). In this context, the experimentally derived stresses serve as input for the simulation whereas the displacements are chosen as target values. We did not only compare combinations of SEF found in the literature, but also recombinations of their summands.

In order to find a global minimum, a good initial guess is needed. Therefore, material parameters are preconditioned based on their individual influence on the resulting stress-strain curve.

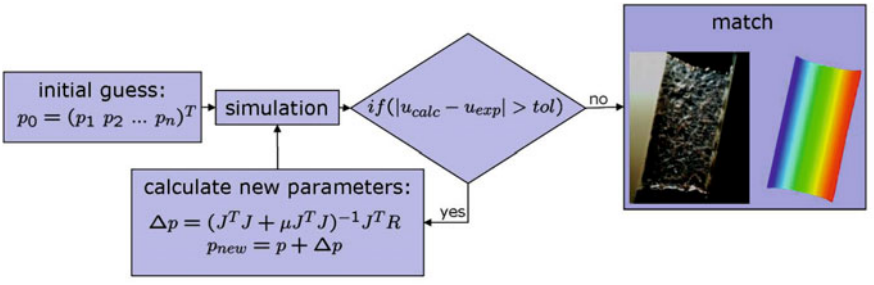

Fig. 6 Flow chart showing the steps of the inverse analysis using a Levenberg-Marquardt algorithm.

The optimal combination of SEF for the constitutive description of lung parenchyma turned out to be

$$W_{par}(\overline{I}_1, J) = c_1\ (\overline{I}_1 - 3)^2 + c_2\ (\overline{I}_1 - 3)^3 + \kappa\ (-2lnJ + J^2 - 1)$$

with the fitted parameters $c_1 = 4.1$ kPa, $c_2 = 20.7$ kPa and $\kappa = 4.1$ kPa. For full details of the experimental studies, the inverse analysis and the examined material models see Rausch et al. (2010b).

3.2 Multi-scale Parenchyma Model

At certain hotspots in our parenchyma model, we want to zoom in on the alveolar micro-structure in order to quantify local stresses and strains relevant for VILI. To bridge the gap between the global parenchyma and the local alveolar level, we have developed a novel computational multi-scale approach based on the nested solution of the boundary value problems (BVP) on both levels. The benefit of this strategy if twofold; firstly, improved homogenised parenchyma properties are derived based on a detailed modeling of the underlying complex micro-structure. Secondly, the global parenchyma model figuratively serves as an "embedding" of locally resolved acinar structures, thereby providing physiologically reasonable boundary conditions for alveolar simulations.

Our approach extends existing methods (Feyel and Chaboche 2000; Kouznetsova et al. 2001; Miehe 2003) to coupled and dynamic scenarios inherent to (mechanical) ventilation. To account for the transient effects, we propose to couple a dynamic simulation on the parenchyma level locally with a quasi-static simulation of the discretised alveolar level. This procedure enables us to investigate the time-dependent behaviour of lung parenchyma as a whole and local alveolar ensembles simultaneously without necessitating to resolve the alveolar micro-structure completely.